Ab Initio Models for Receptor–Ligand Interactions in Proteins. 3. Model Assembly Study of the Proton Transfer in the Hydroxylation Step of the Catalytic Mechanism of *p*-Hydroxybenzoate Hydroxylase

Mikael Peräkylä and Tapani A. Pakkanen*

Contribution from the Department of Chemistry, University of Joensuu, P.O. Box 111, 80101 Joensuu, Finland

Received February 22, 1993®

Abstract: Proton transfer in the hydroxylation step of the catalytic mechanism of *p*-hydroxybenzoate hydroxylase was investigated using the *ab initio* model assembly approach. In the hydroxylation step the hydroxy group is introduced at the ortho position of *p*-hydroxybenzoate. The calculations showed, in accordance with the experimental observations, that ionization of the *p*-hydroxybenzoate is energetically feasible. The role of individual amino acid residues forming hydrogen bonds with the ligand was investigated energetically, and the residues were calculated to stabilize the ionized form of *p*-hydroxybenzoate. The calculations also supported the conclusion that the intermediate in the hydroxylation is the radical OH adduct of *p*-hydroxybenzoate.

Introduction

Ab initio quantum mechanical methods can be used to obtain information about the electronic structure of molecules or reaction intermediates which is difficult or even impossible to obtain experimentally. One area where quantum mechanical methods have proven useful is in the simulation of enzyme reactions using model systems based on the X-ray crystal structure of the enzyme.[1-5] In such calculations, model compounds are normally used to construct the active-site model. If results are to be reliable, these model compounds must be electrostatically and sterically similar to the species they are modeling. In earlier studies,[6,7] we developed model compounds that reproduce the electrostatic and steric properties of amino acids and a study was made of the applicability of the model compound approach in general. Here the model compound approach is applied to study the enzyme reaction of *p*-hydroxybenzoate hydroxylase (PHBH).

PHBH is a monooxygenase flavoenzyme that catalyzes the conversion of *p*-hydroxybenzoate (*p*-OHB) to 3,4-dihydroxybenzoate (3,4-DOHB) using molecular oxygen and nicotinamide adenine dinucleotide phosphate (NADPH):

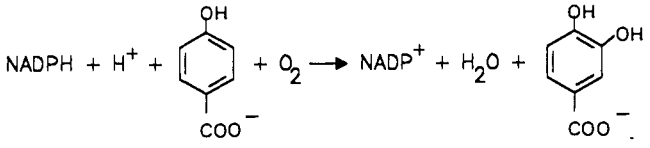

The numbering of the atoms of *p*-OHB, 3,4-DOHB, and the flavin ring is presented in Figure 1. Several X-ray structures of PHBH have been determined,[8-13] and the enzyme reaction has been extensively studied by spectroscopic,[14-19] kinetic,[20-25] and chemical modification[26-28] studies. Studies of model reactions

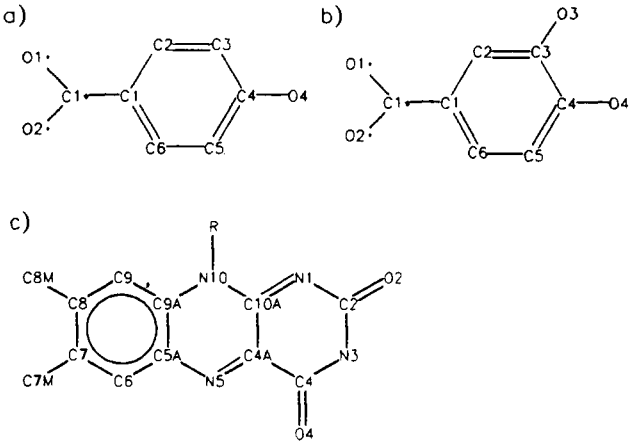

Figure 1. Atomic numbering of (a) *p*-OHB, (b) 3,4-DOHB, and (c) flavin.

® Abstract published in *Advance ACS Abstracts,* October 15, 1993.

(1) Weiner, S. J.; Seibel, G. L.; Kollman, P. A. *Proc. Natl. Acad. Sci.* U.S.A. **1986**, *83*, 649.
(2) Alagona, G.; Desmeules, P.; Ghio, C.; Kollman, P. A. *J. Am. Chem. Soc.* **1984**, *106*, 3623.
(3) Bolis, G.; Ragazzi, M.; Salvaderi, D.; Ferro, D. R.; Clementi, E. *Gazz. Chim. Ital.* **1978**, *108*, 425.
(4) Waszkowycz, B.; Hillier, I. H.; Gensmantel, N.; Payling, D. W. *J. Chem. Soc., Perkin Trans. 2* **1991**, 2025.
(5) Liang, J.-Y.; Lipscomb, W. N. *Biochemistry* **1989**, *28*, 9724.
(6) Lindroos, J.; Peräkylä, M.; Björkroth, J.-P.; Pakkanen, T. A. *J. Chem. Soc., Perkin Trans. 2* **1992**, 2271.
(7) Peräkylä, M.; Pakkanen, T. A. *J. Chem. Res.*, in press.
(8) Wierenga, R. K.; de Jong, R. J.; Kalk, K. H.; Hol, W. G. J.; Drenth, J. *J. Mol. Biol.* **1979**, *131*, 55.
(9) Weijer, W. J.; Hofsteenge, J.; Beintema, J. J.; Wierenga, R. K.; Drenth, J. *Eur. J. Biochem.* **1983**, *133*, 109.
(10) Schreuder, H. A.; van der Laan, J. M.; Hol. W. G. J.; Drenth, J. *J. Mol. Biol.* **1988**, *119*, 637.
(11) Schreuder, H. A.; Prick, P. A. J.; Wierenga, R. K.; Vriend, G.; Wilson, K. S.; Hol, W. G. J.; Drenth, J. *J. Mol. Biol.* **1989**, *208*, 679.
(12) van der Laan, J. M.; Schreuder, H. A.; Swarte, M. B. A.; Wierenga, R. K.; Kalk, K. H.; Hol, W. G. J.; Drenth, J. *Biochemistry* **1989**, *28*, 7199.
(13) Schreuder, H. A.; van der Laan, J. M.; Swarte, M. B. A.; Kalk, K. H.; Hol, W. G. J.; Drenth, J. *Proteins* **1992**, *14*, 178.
(14) Shoun, H.; Beppu, T.; Arima, K. *J. Biol. Chem.* **1979**, *254*, 899.
(15) Shoun, H.; Higashi, N.; Beppu, T.; Nakamura, S.; Hiromi, K.; Arima, K. *J. Biol. Chem.* **1979**, *254*, 10944.
(16) Wessiak, A.; Noar, J. B.; Bruice, T. C. *Proc. Natl. Acad. Sci. U.S.A.* **1984**, *81*, 332.
(17) Beinstock, R. J.; Schopfer, L. M.; Morris, M. D. *J. Am. Chem. Soc.* **1986**, *108*, 1833.
(18) Anderson, R. F.; Patel, K. B.; Stratford, M. R. L. *J. Biol. Chem.* **1987**, *262*, 17475.
(19) Schopfer, L. M.; Wessiak, A.; Massey, V. *J. Biol. Chem.* **1991**, *266*, 13080.
(20) Entsch, B.; Ballou, D. P.; Massey, V. *J. Biol. Chem.* **1976**, *251*, 2550.
(21) Entsch, B.; Ballou, D. P.; Husain, M.; Massey, V. *J. Biol. Chem.* **1976**, *251*, 7367.
(22) Ghisla, S.; Entsch, B. Massey, V.; Husein, M. *Eur. J. Biochem.* **1977**, *76*, 139.
(23) Husain, M.; Entsch, B. Ballou, D. P.; Massey, V. Chapman, P. J. *J. Biol. Chem.* **1980**, *255*, 4189.
(24) Husain, M.; Massey, V. *J. Biol. Chem.* **1979**, *254*, 6657.

0002-7863/93/1515-10958$04.00/0

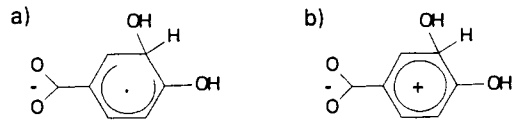

Figure 2. (a) 3-OH radical and (b) 3-OH adduct of *p*-OHB.

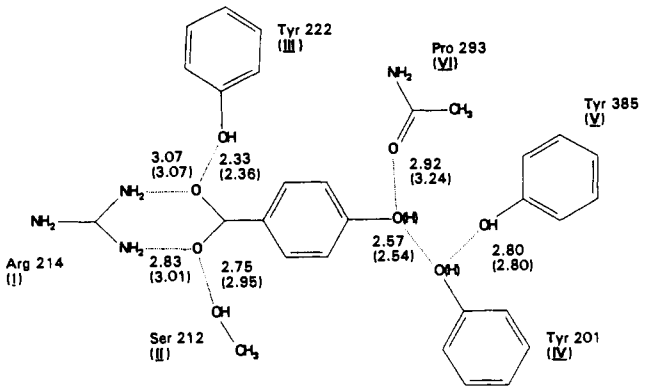

Figure 3. Hydrogen-bonding distances between *p*-OHB (and 3,4-DOHB) and amino acid residues in the active site of PHBH.[11] Distances in the PHBH–3,4-DOHB complex are in parentheses.

have provided still further insight into the enzyme reaction.[29,30] On the basis of these studies, the overall catalytic cycle has been presented.[31] The catalytic cycle consists of reductive and oxidative half-reactions with six ordered steps. In the reductive half-reaction after the binding of *p*-OHB (step 1), the cofactor flavin is reduced by NADPH (step 2). The oxidative half-reaction consists of at least three intermediates (**I–III**). In the oxidative half-reaction after the release of oxidized $NADP^+$, flavin is oxygenated by molecular oxygen (step 3) to C(4a)-flavin hydroperoxide (**I**). In the following hydroxylation step (step 4), oxygen is transferred from C(4a)-flavin hydroperoxide to the aromatic ring of the substrate through intermediate **II**, resulting in C(4a)-flavin hydroxide (**III**, step 5). The catalytic cycle is terminated by the release of the product and the other oxygen of O_2 in the form of water (step 6). In contrast to the case for species **I** and **III**, there is no general agreement about the structure of intermediate **II**. Spectral studies suggest that the spectrum of **II** is a composite, with the 3-hydroxyl radical adduct of the substrate (the hydroxycyclohexadienyl radical of the substrate) as one component (Figure 2a). The spectrum of intermediate **II** exhibits a pH dependence due to the substrate component of the specturm, which has a pk_a value of 7.8. This spectral change has been argued to be due to the ionization of the intermediate.[19]

The hydroxylation step of the oxidative half-reaction is investigated in the following. Since the hydroxylation step is electrophilic in nature, one would expect it to be facilitated by a deprotonated 4-O^- group of *p*-OHB. The pk_a of 4-OH of *p*-OHB in the enzyme is 7.4.[28] Lying in the active site are Tyr-201 and Tyr-385, which form a hydrogen-bond network with the 4-OH of *p*-OHB (Figure 3) and are involved in the ionization of the ligand. Tyr-201 is directly hydrogen bonded to 4-OH, while Tyr-385 forms a hydrogen bond to OH of Tyr-201.

Chemical modification and site-directed mutation studies have indicated that one of the tyrosine residues in the active site, most probably tyrosine 201, is ionized ($pk_a = 7.7–7.9$).[32] Furthermore, the mutant Tyr-201 → Phe was found to have only 6% of the catalytic activity of the wild-type enzyme and to lack the ionization of the substrate. The mutant Tyr-385 → Phe also reduced the catalytic rate, but the ionization of the substrate remained.[28] Thus, ionization of the substrate is probably needed to activate the substrate, and Tyr-201 and Tyr-385 are instrumental in the activity of the enzyme. 2,4-Dihydroxybenzoate and 3-fluoro-*p*-hydroxybenzoate, which likewise are hydroxylated by PHBH, contain a similar ionizable 4-OH group.[20,24]

The aim of the present *ab initio* model assembly study is to investigate the proton transfer from the 4-OH site of the ligand to the ionized Tyr-201 in the complexes of PHBH with substrate *p*-OHB (**1**, **2**), with 3-OH radical adducts (**5**, **6**) and 3-OH adducts (**7**, **8**) of the substrate (these adducts being possible structures of *p*-OHB in the intermediate **II**) and with product 3,4-DOHB (**3**, **4**). To shed light on the mechanism of the hydroxylation, the calculated energetics of the proton-transfer reactions are compared with the experimental results. The role of the amino acid residues forming hydrogen bonds to *p*-OHB is investigated to find out how the pk_a of *p*-OHB is lowered from 9.3 in the free molecule to 7.4 in the enzyme.

Computational Details

Ab initio molecular orbital calculations were carried out with the Gaussian 90[33] and Gaussian 92[34] programs on SGI 4D/35, Stellar DS2000, and Cray X-MP EA/432 computers. Calculations of the complexes were made by the direct SCF method.[35] In the direct single-point calculations, default accuracies of Gaussian were used for integrals (10^{-6}) and for the convergence of SCF (either 10^{-4} on both the energy and the density or 10^{-5} on the energy, whichever comes first). Restricted Hartree–Fock wave functions were calculated for closed-shell systems. In dealing with open-shell systems, the unrestricted Hartree–Fock method was employed.

For the phenol, the basis set splicing technique was applied to reduce the size of the 3-21G calculation.[6,36–38] Here the three carbon and hydrogen atoms farthest from the OH group were calculated using the STO-3G basis set, while the 3-21G was used for the other atoms. The basis set with spliced phenols will be denoted as 3-21G(spl). This procedure was earlier tested in phenol–methanol interaction calculations.[6] Otherwise standard basis sets of Gaussian were employed. Since diffuse functions are important in the description of anionic species,[39,40] the 3-21+G and 6-31+G* were used to obtain gas-phase reference values for the proton-transfer reaction. In the 3-21G(spl) optimization of PHBH–*p*-OHB complexes, all the intermolecular bond lengths and angles between the carbons and oxygens of *p*-OHB were optimized. In the UHF calculations on **7** and **8**, the values of S^2 were 1.16 and 1.01, respectively, showing high spin contamination of the wave functions ($S^2 = 0.75$ for pure doublet). The S^2 values of the model assemblies are close to 1.20 and 1.06 (6-31G*) for the isolated OH radical adducts of *p*-OHB. The effect of spin contamination on energies was studied by comparing the gas-phase energies of the proton transfer from the OH group of *p*-OHB and OH and OH radical adducts of *p*-OHB to phenolate at the various levels (Table I). The proton-transfer energy for the OH radical adduct of *p*-OHB at the 3-21G level is 35.9 kJ/mol higher than that at the UMP2/

(25) Wessiak, A.; Schopfer, L. M.; Massey, V. *J. Biol. Chem.* **1984**, *259*, 12547.
(26) Wijnands, R. A.; Muller, F. *Biochemistry* **1982**, *21*, 6639.
(27) Wijnands, R. A.; Weijer, W. J.; Muller, F.; Jekel, P. A.; van Berkel, W. J. H.; Beintema, J. J. *Biochemistry* **1986**, *25*, 4211.
(28) Entsch, B.; Palfey, B. A.; Ballou, D. P.; Massey, V. *J. Biol. Chem.* **1991**, *266*, 17341.
(29) Kemal, C.; Bruice, T. C. *J. Am. Chem. Soc.* **1979**, *101*, 1635.
(30) Akiyama, T.; Simeno, F.; Murakami, M.; Yoneda, F. *J. Am. Chem. Soc.* **1992**, *114*, 6613.
(31) Schreuder, H. A.; Hol, W. G. J.; Drenth, J. *J. Biol. Chem.* **1988**, *263*, 3131.
(32) Van Berkel, W. J. H.; Muller, F. *Eur. J. Biochem.* **1989**, *179*, 307.
(33) Frisch, M. J.; Head-Gordon, M.; Trucks, G. W.; Foresman, J. B.; Schleger, H. R.; Raghavachari, K.; Robb, M.; Binkley, J. S.; Gonzales, C.; Defrees, D. J.; Fox, D. J.; Whiteside, R. A.; Seeger, R.; Melius, C. F.; Baker, J.; Martin, R. L.; Kahn, R. L.; Stewart, J. J. P.; Topiol, S.; Pople, J. A. *Gaussian 90*; Gaussian Inc.: Pittsburg, PA, 1990.
(34) Frisch, M. J.; Trucks, G. W.; Head-Gordon, M.; Gill, P. M. W.; Wong, M. W.; Foresman, J. B.; Johnson, B. G.; Schlegel, H. B.; Robb, M. A.; Replogle, E. S.; Gomperts, R.; Andres, J. L.; Raghavachari, K.; Binkley, J. S.; Gonzalez, C.; Martin, R. L.; Fox, D. J.; Defrees, D. J.; Baker, J.; Stewart, J. J. P.; Pople, J. A. *Gaussian 92*, Revision B; Gaussian, Inc.: Pittsburgh, PA, 1992.
(35) Almlöf, J.; Faegri, K., Jr.; Korsell, K. *J. Comput. Chem.* **1982**, *3*, 385.
(36) Schmidt, M. W.; Angus, R. O., Jr.; Johnson, R. P. *J. Am. Chem. Soc.* **1982**, *104*, 6838.
(37) Pardo, L.; Mazurek, A. P.; Osman, R. *Int. J. Quantum Chem.* **1990**, *37*, 701.
(38) Jensen, J. H.; Gordon, M. S. *J. Comput. Chem.* **1991**, *12*, 421.
(39) Hehre, W. J.; Radom, L.; Schleyer, P. v. R. *Ab Initio Molecular Orbital Theory*; John Wiley and Sons: New York, 1985; p 310.
(40) Clark, T.; Chandrasekhar, J.; Spitznagel, G. W.; Schleyer, P. v. R. *J. Comput. Chem.* **1983**, *4*, 294.

Table I. Energies for the Proton Transfer (ΔE, kJ/mol) from the OH group of *p*-OHB and OH and OH Radical Adducts of *p*-OHB to Phenolate in the Gas Phase[a]

	ΔE					
proton donor	3-21G (spl)	3-21G	3-21+G	6-31G*	6-31+G*	MP2/6-31G*//6-31G* [b]
p-OHB	227.7	286.1	249.4	280.4	264.6	293.3
OH adduct of *p*-OHB		−364.8		−345.0		−342.9
OH radical adduct of *p*-OHB		241.4		245.2		205.5 (231.4)

[a] Positive ΔE values indicate endothermic proton transfer from *p*-OHB compounds to phenolate. [b] UMP2/6-31G*//6-31G* and PUMP2/6-31G*//6-31G* (in parentheses) energies for the OH radical adduct.

6-31G*//6-31G* level, and after projection of the quartet contaminant from the UMP2 wave function (PUMP2), the difference is 10.0 kJ/mol. The 3-21G values for *p*-OHB and the OH adduct of *p*-OHB also agree reasonably with the MP2/6-31G*//6-31G* energies. These results indicate that the conclusions based on the 3-21G proton-transfer energies of the model assemblies are at least qualitatively correct.

Construction of the Active-Site Model

The crystal structure of PHBH complexed with its reaction product 3,4-DOHB[10] was retrieved from the Data Bank[41] at Brookhaven National Library (entry name 1PHH). All manipulation of the protein structures and displaying of the results were done with the program O[42] and SYBYL 5.51.[43] The model assemblies of enzyme–*p*-OHB and enzyme–intermediate complexes were constructed by replacing the 3,4-DOHB of the crystal structure by the substrate *p*-OHB or the intermediates. This was done by least-squares fitting of the molecules on 3,4-DOHB. The carbon and oxygen atoms of the aromatic ring and of the CO_2^- and 4-OH groups were used in the fitting procedure. The structures of *p*-OHB and 3,4-DOHB used in the fitting were fully optimized, as were the structures of the intermediates, except the torsion of the hydrogen of 3-OH which was set to 78°. At this value the hydrogen of 3-OH points toward the carbonyl oxygen of Pro-293. The amino acid residues Arg-214 (residue **I**), Ser-212 (**II**), Tyr-222 (**III**), Tyr-201 (**IV**), and Pro-293 (**VI**), which make hydrogen bonds to the ligand molecules and Tyr-385 (**V**), were taken into the model assembly. Phenol was used as a model compound for tyrosines, methanol for serine, acetamide for the main chain atoms of proline, and the guanidium cation for arginine. The geometries of the model compounds were optimized at the same level as the calculations of the complexes were done. The hydrogen-bonding distances between the amino acid residues and the ligand molecules in the PHBH–*p*-OHB and PHBH–3,4-DOHB model assemblies were adjusted to the values in the X-ray structures of the corresponding complexes determined at 1.9-Å resolution.[12]

Results and Discussion

Proton Transfer in the *p*-OHB and 3,4-DOHB Complexes and the Receptor–Ligand Interactions. The results for the proton-transfer reaction *p*-OHB + phenolate anion → *p*-OB^- + phenol (Table I) show that the reaction is highly endothermic in the gas phase, being 264.6 kJ mol^{-1} at the 6-31+G* and 293.3 kJ mol^{-1} at the MP2/6-31G*//6-31G* level. The 3-21G value of 286 kJ mol^{-1} is closer to these values than is the 3-21G(spl) value of 227.7 kJ mol^{-1}. The proton-transfer energy in the gas phase for *p*-OHB + phenol → *p*-OB^- + phenol cation is 1027.1 kJ mol^{-1} at the 3-21G level. Although the 3-21G energy would have been changed substantially if the surrounding amino acid residues had been included, the result indicates that the proton transfer in the enzyme from the substrate's 4-OH to the oxygen of Tyr-201 is energetically feasible only if Tyr-201 is ionized.

The calculated energies for the proton-transfer reaction PHBH–*p*-OHB (**1**) → PHBH–*p*-BH^- (**2**) in the model assemblies (Figures 4 and 5) are shown in Table II. The proton-transfer energy for **1** → **2** calculated from the nonoptimized complexes is 29.2 kJ mol^{-1} at the 3-21G level. It is 21.8 kJ mol^{-1} smaller at the 3-21G(spl) level, showing thereby the same dependence on the basis set as for the gas-phase reaction. The calculated energy for the proton transfer from the 4-OH of the product 3,4-DOHB to the ionized Tyr-201 (reaction **3** → **4**) is 28.7 kJ mol^{-1} (3-21G). As expected, this is close to the proton-transfer energy of *p*-OHB and predicts that the pK_a for 3,4-DOHB in the enzyme is about 7.4. After the optimizations of **1** and **2**, the proton transfer becomes less favored by 12 kJ mol^{-1} at the 3-21G(spl) level. The optimizations changed most the bond lengths and angles of the CO_2^- group and the C1–C1* bond length. In **1** and **2** the C1*–O2* lengths increased at the 3-21G(spl) level by 0.05 Å, while the C1*O1* lengths were unchanged. This dissimilar behavior is probably due to the difference in the hydrogen-bond distances, and thus the hydrogen-bond strengths between Arg-214 and O1* and O2*. The O1*–Arg-214 and O2*–Arg-214 hydrogen bonds are 3.07 and 2.83 Å, respectively. Optimizations decreased the C1–C1*–O1* and C1–C1*–O2* angles by 3–7°, and the C1–C1* distances increased 0.07 Å in **1** and **2**. Otherwise the optimizations caused changes

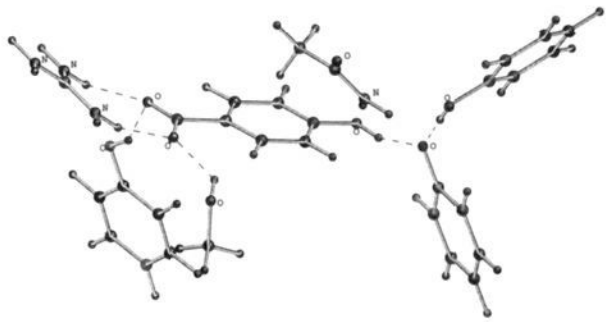

Figure 4. PHBH–*p*-OHB model assembly (**1**).

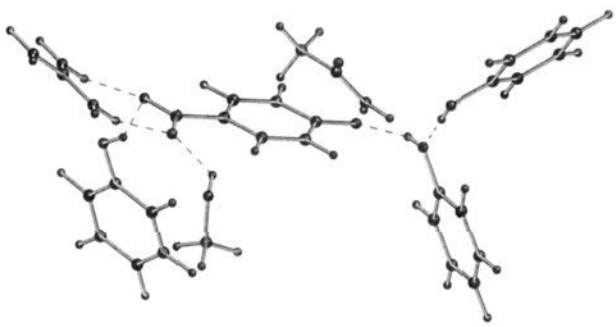

Figure 5. PHBH–*p*-OB^- model assembly (**2**).

Table II. Absolute Energies (au) of 1–4 and Energies (kJ mol^{-1}) for the Proton-Transfer Reaction 1 → 2 at the 3-21G(spl) and 3-21G Levels and for 3 → 4 at the 3-21G Level[a]

	3-21G(spl)	3-21G
1	−1923.487 24	−1925.722 23
2	−1923.479 71	−1925.711 09
1 → **2**	7.4 (19.8)	29.2
3		−2000.161 80
4		−2000.150 85
3 → **4**		28.7

[a] The STO-3G energies for **1** → **2** are 52.4 kJ/mol for the nonoptimized and 63.5 kJ/mol for the optimized complexes.

(41) Bernstein, F. C.; Koetzle, T. F.; Williams, G. J. B.; Meyer, E. F., Jr.; Brice, M. D.; Rodgers, J. R.; Kennard, O.; Shimanouchi, T.; Tasumi, M. *J. Mol. Biol.* **1977**, *112*, 535.

(42) Jones, T. A.; Zou, J.-Y.; Cowan, S. W. *Acta Crystallogr.* **1991**, *A47*, 110.

(43) SYBYL, version 5.51; Tripos Associates, Inc.: St. Louis, MO.

Table III. Energies (kJ mol^{-1}) for the Proton Transfer without Selected Residues and the Changes in Energy Compared with the Reaction 1 → 2 (29.2 kJ/mol) at the 3-21G Level[a]

excluded residue	proton-transfer energy	ΔE
I	90.3	61.1
II	42.1	12.9
III	47.2	17.9
V	5.3	−34.5
VI	14.3	−14.9
II + III	60.6	31.3
I + II + III + V + VI	79.5	50.3

[a] See Figure 3 for definition of the residues.

Table IV. Interaction Energies (kJmol^{-1}) of the Residues I–III, V, VI, and II + III in Complexes 1 and 2 at the 3-21G Level[a]

	interaction energy	
residue	**1**	**2**
I	−605.1	−666.2
II	−34.4	−47.3
III	−33.2	−51.1
V	−110.2	−75.7
VI	25.4	40.3
II + III	−74.0	−105.3

[a] See Figure 3 for definition of the residues.

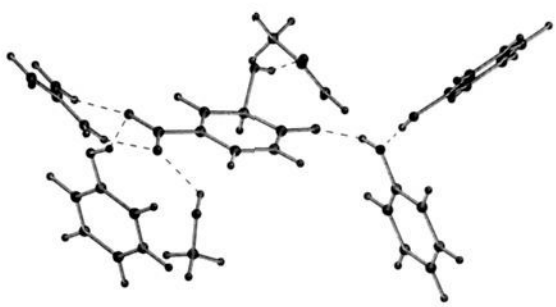

Figure 6. PHBH–3-OH radical adduct model assembly (**6**).

in the geometries equal to 0.01–0.02 Å in bond distances and 1–2° in bond angles.

The results above show, in accordance with the experimental observations, that the proton transfer in the PHBH–*p*-OHB complex (**1** → **2**) is energetically feasible. Next the effects of the hydrogen-bonding residues **I**–**VI** on the proton transfer were studied by calculating the energy of the proton transfer in the PHBH–*p*-OHB model assemblies (**1** and **2**) without selected residues (Table III). The interaction energies of each residue before and after the proton transfer were also calculated (Table IV). Calculations were made at the 3-21G level.

It has been argued that Pro-293 and Thr-294 make the proton transfer unfavorable because of the partial negative charges of their carbonyl oxygens, which are located near the ionizable 4-OH of *p*-OBH.[44] In the model, the carbonyl oxygen of Pro-293 (residue **VI**) is located 2.92 Å from the O4. The Pro-293 is also close to C3 where the hydroxyl group is introduced in the enzyme reaction. In the PHBH–3,4-DOHB complex (**3**) the oxygen of Pro-293 is 2.35 Å from the oxygen of 3-OH. Because of the proximity to C3, Pro-293 may be of importance in the activation of C3 and in the stabilization of the transition state of the enzyme reaction (Figure 6). In the PHBH–*p*-OHB complex (**1**, Figure 4), the distance between the carbonyl oxygen of Thr-294, which is not included in the model, and O4 is 2.97 Å. We can see from Table IV that exclusion of residue **VI** (Pro-293) from the model assembly facilitates the proton transfer by 14.9 kJ mol^{-1}. The interaction energy of **VI** is repulsive in both complexes, being 25.4 kJ mol^{-1} in **1** and 40.3 kJ mol^{-1} in **2**.

(44) Schreuder, H. A.; Hol, W. G. J.; Drenth, J. *Biochemistry* **1990**, *29*, 3101.

Molecular electrostatic potential maps (MEP) calculated at the 3-21G level in the plane of the aromatic ring of *p*-OHB and *p*-OB$^-$ are presented in Figure 7. The partial charges of the ring heavy atoms of *p*-OBH and *p*-OB$^-$ obtained from Mulliken population analysis[45] and Natural Bond Orbital (NBO) analysis[46] are listed in Table V. The MEPs and partial charges show that the negative charge is spread from the ionized O4 along the π-system of the ligand to the opposite end of the molecule. The negative charges of O1* and O2* have increased by 0.016 (Mulliken) and 0.020 (NBO). In addition to the increased negative charge around the CO_2^-, two additional features of the MEPs can be seen. First, owing to the ionization of 4-OH, the negative regions in the vicinity of the ortho and meta carbons of the ligand are considerably enlarged. This indicates that the ionization has made the ligand more prone to electrophilic attack, which evidently facilitates the enzyme reaction. Second, the electrostatic potential in the region between O4 and the carbonyl oxygen of **VI** (Pro-293) is enlarged. This is in accordance with the calculated effect of **VI** on the proton-transfer reaction and the increase in the repulsive interaction of **VI** (14.3 kJ mol^{-1}). The ionization makes the interactions of residues **I**–**III**, which form hydrogen bonds to the CO_2^- group of *p*–OHB (Table IV), more attractive. The ion–pair interaction energy between residue **III** (Arg-214) and the ligand has increased by 61.1 kJ mol^{-1}. The interaction energy of **II** (Ser-212) has increased by 12.9 kJ mol^{-1}, and the energy of **III** (Tyr-222), by 17.9 kJ mol^{-1}. The higher increase in the interaction of **III** may be influenced by the fact that the aromatic ring in **III** is more polarizable and can delocalize the charge in the aromatic π-system better than methanol. Also relevant is the shorter hydrogen-bond distance from the carboxylate oxygen to **III** (2.33 and 2.36 Å) than to **II** (2.75 and 2.95 Å). It may be noted, in addition, that the interaction energies of **II** and **III** in the complexes are not additive. The nonadditivities are 6.4 and 6.9 kJ mol^{-1} in complexes **1** and **2**, respectively. Thus, the exclusion of one ligand is partly compensated by the stronger interaction of the other.

The delocalization of the negative charge and the stabilization of the ionized *p*-OB$^-$ have considerable effect on the lowering of the proton-transfer energy. The exclusion of residue **II** and **III** makes the proton transfer more endothermic. As expected on the basis of the higher interaction energy, the effect of excluding **III** is larger. When both residues are excluded at the same time, the proton transfer becomes 31.3 kJ mol^{-1} more endothermic. In the model from which all the residues except **IV** are excluded, leaving only the proton-transfer partners in the model, the proton-transfer energy is 79.5 kJ mol^{-1}. Although this energy is 206.6 kJ mol^{-1} lower than the energy of the gas-phase reaction, it is still considerable. The observation that the proton transfer becomes more favorable due to the hydrogen-bonding residues is in accordance with the general idea that a polarizable environment stabilizes species with charges.[47–49] Here this phenomenon is observed not only as the delocalization of the charge but also as stronger hydrogen bonds between the CO_2^- group and ligands **I**–**III**.

In spite of high attractive interaction energies, residue **V** (Tyr-385) has an unfavorable effect on the proton-transfer reaction. The exclusion of **V** makes the proton-transfer reaction 34.5 kJ mol^{-1} more favorable. The reason is clear: **V** makes a hydrogen bond to residue **IV** (Tyr-201) and stabilizes the ionized form of **IV**. However, through this stabilization, **V** (Tyr-385) may have an important role in lowering the pk_a of Tyr-201 to the value of 7.7–7.9[32] in the enzyme.

(45) Mulliken, R. S. *J. Chem. Phys.* **1955**, *23*, 1833.
(46) Foster, J. P.; Weinhold, F. *J. Am. Chem. Soc.* **1980**, *102*, 7211.
(47) Tapia, O.; Cardenas, R.; Andres, J.; Krechl, J.; Campillo, M.; Colonna-Cesari, F. *Int. J. Quantum Chem.* **1991**, *39*, 767.
(48) Solà, M.; Lledós, A.; Duran, M.; Bertrán, J.; Abboud, J.-L. M. *J. Am. Chem. Soc.* **1991**, *113*, 2873.
(49) Wong, M. W.; Frisch, M. J.; Wiberg, K. B. *J. Am. Chem. Soc.* **1991**, *113*, 4776.

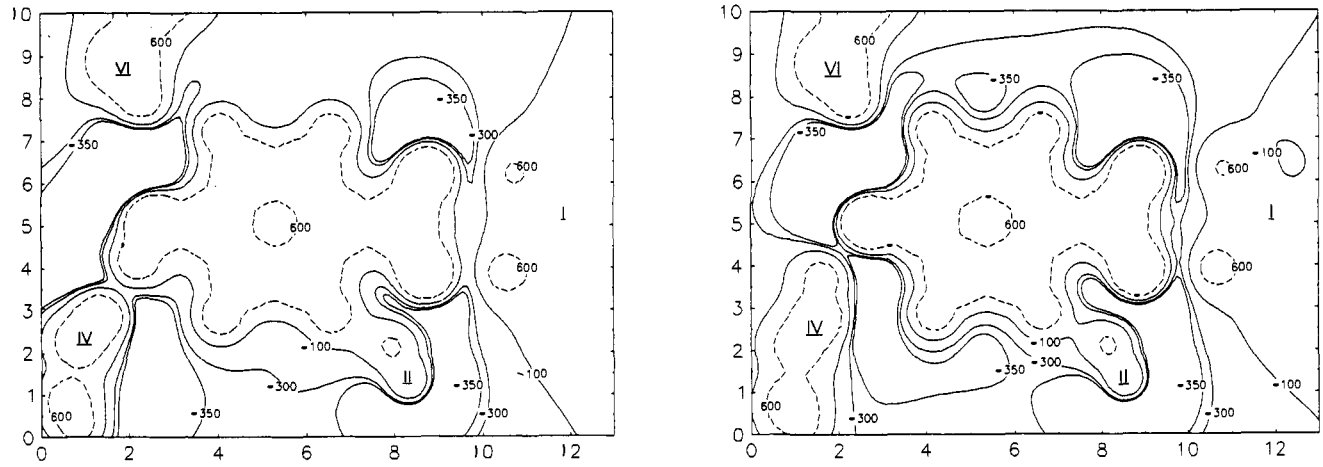

Figure 7. Molecular electrostatic potential in the plane of the aromatic ring of the ligand in (a, left) PHBH–*p*-OHB (**1**) and (b, right) PHBH–*p*-OB$^-$ (**2**) model assemblies calculated at the 3-21G level. Values of the isocontours are in kJ mol^{-1}, and the positive isocontours (600 kJ mol^{-1}) are drawn with dashed lines. The values of the axes are in angstroms.

Table V. Calculated Mulliken Charges for Selected Atoms of *p*-OHB and *p*-OB$^-$ in Complexes 1 and 2 at the 3-21G(spl) and 3-21G Levels and Charges from NBO Analysis at the 3-21G Level[a]

	Mulliken charges		NBO charges
	3-21G(spl)	3-21G	3-21G
	p-OHB (**1**)		
C1	−0.293 (−0.311)	−0.295	−0.268
C2	−0.204 (−0.184)	−0.205	−0.179
C3	−0.296 (−0.295)	−0.292	−0.322
C4	0.375 (0.423)	0.374	0.387
C5	−0.304 (−0.314)	−0.302	−0.352
C6	−0.211 (−0.194)	−0.210	−0.167
O4	−0.788 (−0.801)	−0.787	−0.744
C1*	0.954 (0.927)	0.954	0.921
O1*	−0.774 (−0.769)	−0.771	−0.817
O2*	−0.780 (−0.794)	−0.782	−0.829
	p-OB$^-$ (**2**)		
C1	−0.325 (−0.345)	−0.331	−0.347
C2	−0.197 (−0.178)	−0.198	−0.162
C3	−0.336 (−0.336)	−0.332	−0.403
C4	0.479 (0.491)	0.483	0.490
C5	−0.336 (−0.340)	−0.336	−0.414
C6	−0.201 (−0.188)	−0.200	−0.154
O4	−0.836 (−0.826)	−0.838	−0.817
C1*	0.925 (0.902)	0.925	0.915
O1*	−0.790 (−0.789)	−0.787	−0.837
O2*	−0.796 (−0.810)	−0.798	−0.849

[a] Charges of the optimized complexes are in parentheses.

The experiments with various substrate analogues, and the location of the site of the hydroxylation ortho to the existing OH, establish that the hydroxylation proceeds by an electrophilic attack.[44] The ionization of 4-OH, which makes the 3-position more prone to electrophilic attack, also has been observed to facilitate the hydroxylation.[28] The Mulliken and NBO charges of ring carbon atoms C1–C6 of *p*-OHB and *o*-OB$^-$ (Table V) show the activation of ortho positions 3 and 5 by the OH group and the activating effect of the ionization of 4-OH. At the 3-21G level, the meta carbons have Mulliken negative charges that are 0.09 and 0.14 smaller than the ortho carbons in *p*-OHB and *p*-OB$^-$, respectively. In the NBO analysis these values are 0.16 and 0.25. The optimizations can be seen to have increased the difference between the charges of the ortho and meta carbons by 0.013–0.020. The MEPs reproduce the tendencies observed in atomic partial charges.

Proton-Transfer Reactions in the Complexes of Intermediates. The structure of *p*-OHB and its analogues in the intermediate **II** is argued to be either a 3-OH radical adduct (Figure 2a) or a 3-OH adduct (Figure 2b) of the substrate.[18,19,50,51] Both adducts are easily fitted to the active site. The aromatic rings of both

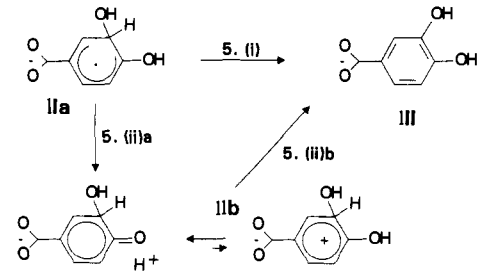

Figure 8. Two alternative routes for the conversion of **II** to **III**.

Table VI. Absolute Energies (au) of 5–8 and Energies (kJ mol^{-1}) for the Proton-Transfer Reactions 5 → 6 and 7 → 8 at the 3-21G Level

	3-21G	reaction	proton-transfer energy
5	−2000.700 53		
6	−2000.677 75	**5** → **6**	59.8
7	−2000.616 23		
8	−2000.675 41	**7** → **8**	−155.4

species are almost planar, and the 3-OH can form a hydrogen bond to the Pro-293, which would stabilize the intermediate. The structure of the 3-OH radical adduct of *p*-OB$^-$ fitted to the active site is shown in Figure 6. Spectral studies have indicated that the substrate may be a radical.[18,50] However, the possibility of a 3-OH adduct is not ruled out, first, because no unpaired electron has been observed in the intermediate **II** and, second, because the spectrum of this adduct, which could be formed upon the oxidation of the radical species (Figure 8, step 5, (ii)a), would be very similar to that of the radical.[50]

Since the spectrum of **II** exhibits a pH dependence with pk_a = 7.8 due to the substrate component of the spectrum,[19] the energetics of the proton transfer was investigated for models of 3–OH radical adducts (**5** → **6**) and 3–OH adducts (**7** → **8**) of *p*-OHB to determine which one better is suited to the observed pk_a. The results from proton-transfer calculations at the 3-21G level are presented in Table VI.

If we calibrate the calculated energies by assuming that the proton-transfer energy 0.0 kJ mol^{-1} corresponds to pk_a = 7.0, and the 29.2 kJ mol^{-1} calculated for **1** → **2** corresponds to the observed pk_a = 7.4, then the proton-transfer energy for the intermediate **II** with pk_a = 7.8 can be predicted to be roughly 60 kJ mol^{-1}

(50) Anderson, R. F. In *Oxidases and Related Redox Systems: Progress in Clinical and Biological Research*; King, T. E., Mason, H. S., Morrison, M., Eds.; Alan R. Liss. Inc.: New York, 1988; p 167, Vol. 274.
(51) Anderson, R. F.; Patel, K. B.; Vojnovic, B. *J. Biol. Chem.* **1991**, *266*, 13086.

($\Delta\Delta E \propto \Delta pk_a$).[52] The calculated energy of 59.8 kJ mol^{-1} for the radical adduct (**5** → **6**) is in excellent agreement with the estimate. In the case of **7** → **8**, the pk_a predicted in a similar way is as low as 5. Despite the many simplifications incorporated into the model, the result firmly indicates that the radical adduct is involved in the intermediate **II**.

There is some spectral evidence to suggest that more than one species is involved in the conversion **II** → **III** in the hydroxylation, as shown in Figure 8.[18,19,50,51] In addition, a small isotope effect (k_H/k_D = 1.10) was observed when 2,4-dihydroxybenzoate was used as a substrate for the conversion **II** → **III**.[45] There are two possible pathways for the decay of intermediate **II** (Figure 8, step 5, (i) and (ii)) which can explain the isotope effect.[51] (i) The hydrogen may be abstracted by a base such as a •H. In this case the isotope effect would be small because the C–H bond is effectively broken before the transition state. (ii) There may be more than one transition state in the conversion **II** → **III**. In this conversion the radical adduct is first oxidized and H^+ is abstracted by the base from the OH adduct. On the basis of the experimental observations and the present calculations, the hydroxylation pathway (i) seems more probable than the second pathway (ii). This conclusion is supported by the fact that the intermediate **IIb**, if it is formed at all, must be very short-lived, decaying rapidly to the intermediate **III**. Hence, it seems unlikely that the isotope effect would have been detected for the conversion **II** → **III** if H^+ were abstracted by a base from the intermediate **IIb**.

Conclusions

This paper has presented *ab initio* model assembly calculations on the proton-transfer reaction between the ligand *p*-OHB and the active-site Tyr-201 in PHBH. The use of several simplifications in the calculations needs to be emphasized. First, the total optimization of the active site has been neglected; second, the possible steric and long-range electrostatic effects of the protein matrix have not been included. Despite these shortcomings, the results of the present calculations are in reasonable agreement with the experimental observations and elucidate several aspects of the enzyme reaction of PHBH.

(52) $\Delta\Delta E \propto \Delta pk_a$ comes from the equation $\Delta\Delta G = 2.3RT\delta pk_a$.

The calculations provide insight into the role of the ligand-binding amino acids in lowering the pk_a of *p*-OHB from the value of 9.3 for the free molecule to the value 7.4 for the enzyme. Owing to the higher negative charges of the carboxylate oxygens in the ionized than in the nonionized form of the ligand, they made stronger hydrogen bonds and so facilitated the proton transfer. The amino acid residues Arg-214, Ser-212, and Tyr-222 forming hydrogen bonds to the CO_2^- group of *p*-OHB were important in this respect. The ionization increased the hydrogen-bonding energies between the ligand and Arg-214, Ser-212, and Tyr-222 by 61.1, 12.9, and 17.9 kJ mol^{-1}, respectively. These results are a manifestation of the general rule that the more highly charged species are stabilized most by a polarizable environment such as protein matrix. Pro-293 made the proton transfer 14.9 kJ mol^{-1} more unfavorable due to the short 2.94-Å distance between the carbonyl oxygen of Pro-293 and the ionizable oxygen of *p*-OHB. The structures of PHBH–intermediate complexes revealed that Pro-293 may have an important role in stabilizing the intermediate **II** by forming a hydrogen bond to the 3-OH of the intermediate.

The calculated proton-transfer energy in the PHBH–*p*-OHB complex was 29.2 kJ mol^{-1} at the 3-21G level and 7.4 kJ mol^{-1} at the 3-21G(spl) level. The partial optimization of the ligand increased the proton-transfer energy by 12 kJ mol^{-1} at the 3-21G(spl) level. The experimental pk_a in this complex is 7.4. The OH radical and OH adducts of *p*-OHB were studied as possible structures of the ligand in the intermediate **II**. The calculated proton-transfer energy was 59.8 kJ mol^{-1} for the OH radical adduct. For the OH adduct it was −155.4 kJ mol^{-1}, indicating that this species would be in ionized form in the enzyme. Comparison of the calculated proton-transfer energies and the observed pk_a = 7.8 of the intermediate **II** supports the argument that the ligand in the intermediate **II** in the catalytic reaction probably has the OH radical adduct structure. Earlier, spectral studies showed an agreement between the spectrum of the radical adduct complex of enzyme and the intermediate **II**. In spite of attempts, however, no unpaired electrons have been observed in the intermediate **II**. Moreover, the mechanism for the decay of intermediate **II** to intermediate **III**, and the possible role of the OH adduct in this mechanism, are as yet unresolved.